Electronic transport in Heusler-type $Fe_2VAl_{1-x}M_x$ alloys (M=B,In,Si)

M. Vasundhara and V. Srinivas*
Department of Physics & Meteorology, Indian Institute of Technology, Kharagpur 721302, India

V. V. Rao
Cryogenic Engineering Centre, Indian Institute of Technology, Kharagpur 721302, India

(Received 7 January 2008; revised manuscript received 23 April 2008; published 10 June 2008)

The temperature variation of electrical resistivity $\rho(T)$ and Seebeck coefficient $S(T)$ of Heusler-type $Fe_2VAl_{1-x}B_x$ $(0 \leq x \leq 1)$ alloys have been investigated. All the studied alloys were crystallized into a single-phase cubic structure with $Fm3m$ space group. The $\rho(T)$ shows a negative temperature coefficient of resistivity (TCR) for the $x=0$ sample, which turns into a positive TCR for the $x=1$ sample; while intermediate compositions show a resistivity minimum at low temperatures (T_{min}) below 50 K. From the analysis of temperature dependence of the electrical resistivity data, we demonstrate a semiconductorlike to metal transition on B substitution in the Fe_2VAl alloy. With a minute substitution of isoelements (B and In) and nonisoelement (Si), S changes drastically in its sign and magnitude accompanied by an appearance of a broad maximum at higher temperatures, which shifts toward high temperatures with increasing concentration of the substituents. These features are indicative of a dramatic modification in the band structures of the Fe_2VAl alloy with the substitution of elements. Although similar changes in ρ and S values with compositions of B-, In-, and Si-substituted Fe_2VAl alloys are observed, the ρ decreases rapidly on B substitution and ultimately attains a metallic behavior, suggesting a true semiconductorlike to metal transition. The strong composition dependence of S and ρ on elemental substitution is attributed to the size, relative positions of the atomic levels and the number of valence electrons of the substituents.

DOI: 10.1103/PhysRevB.77.224415 PACS number(s): 72.15.Eb, 72.15.Jf, 72.15.Gd

I. INTRODUCTION

Heusler compounds of the form X_2YZ, where X and Y are the elements with partly occupied d-electron orbitals and Z is a sp state element, are formed as a cubic ($L2_1$) structure and provide a great variety of transport and magnetic phenomena. Fe_2VAl is one such class of alloys that has been the topic of interest over the past decade because of its rich variety of unusual transport and magnetic properties.[1–4] The most intriguing characteristics of this alloy are: (i) the occurrence of semiconductorlike transport even though it consists of all metallic constituents and (ii) a nonmagnetic ground state in spite of having 50% Fe.[2,5] However, unlike semiconductors, the experimental results of nuclear magnetic resonance, photoemission, and Hall-effect measurements indicate Fe_2VAl as a low carrier density semimetal,[6–8] which was further supported by the theoretically predicted pseudogap of 0.1–0.2 eV at the Fermi level.[9] On the other hand, Guo *et al.*[3] suggested that the hybridization between transition metals and Al-2p states are responsible for such gaps. Furthermore, Weht and Pickett[9] found that the sp states of Al atom have a strong but indirect effect on the formation of the pseudogap and also on the transport properties, which was later confirmed by optical conductivity studies.[10] Other possible mechanisms such as heavy Fermion[11] and spin fluctuations[7,8] had also been suggested in order to explain the anomalous electronic behavior in this system. Recent reports[12–14] show that the doping of quaternary elements such as Si into Fe_2VAl causes a significant decrease in the low-temperature resistivity (ρ) and substantial enhancement of the Seebeck coefficient (S). The excess of valence electrons in p states of a Si atom may be the cause of significant decrease in ρ and drastic changes in S, as S is very sensitive to the electron density at the Fermi level. On the other hand, from the transport studies of Ge-substituted Fe_2VAl alloys, it was suggested that the doping of heavier element does affect the transport properties.[15] Although reduction in ρ and change in temperature coefficient of resistivity (TCR) indicate a nonmetal-metal transition in Fe_2VAl (Si and Ge) alloys, it is not clear whether the $\rho(T)$ behavior can be explained by conventional theories proposed for metallic samples. On the other hand, Fujii *et al.*[16] have performed band-structure calculations on similar alloys, i.e., Fe_2MnZ [Z=Al,Si,P], and found that the Z atom influences the electronic character of the system through hybridization of Z-p states with Fe and Mn-d states. This suggests that the hybridization of Fe-3d electrons with the Al-p electrons might be an important ingredient in the formation of hollows in their density of states (DOS) at E_F. Whether these hollows create an actual gap depends on details of the electronic structure including the relative positions of the atomic levels and the relative sizes of the ionic radius of the atoms, even though the overall band structures are qualitatively similar for sets of related compounds.[16] Now the most pertinent questions are whether the hybridization (of the XY-d states and Z-sp states) alone can account for the observed changes or the size of the atoms/density of the valence electrons (provided by the Z atom) influence the transport behavior. This can be verified by a systematic substitution of quaternary elements, thereby retaining the same electron density. To the best of our knowledge, such studies have not been carried out until now. This has motivated us to study the substitution of isoelectronic elements having different atomic sizes such as a smaller atom "B" and a larger atom "In" at the Al sites. The purpose of the present study is to investigate the effect of relative changes in atomic and electron densities on transport prop-

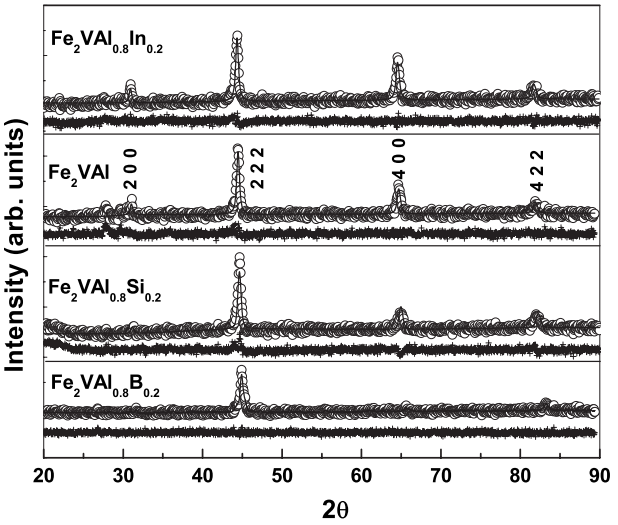

FIG. 1. XRD patterns of Fe_2VAl, $Fe_2VAl_{0.8}B_{0.2}$, $Fe_2VAl_{0.8}Si_{0.2}$, and $Fe_2VAl_{0.8}In_{0.2}$ alloys with Reitveld refinement analysis. The symbol (○) indicates the raw data, the continuous line indicates the fit to the analysis, and the symbol (+) indicates the residue values obtained from the fits.

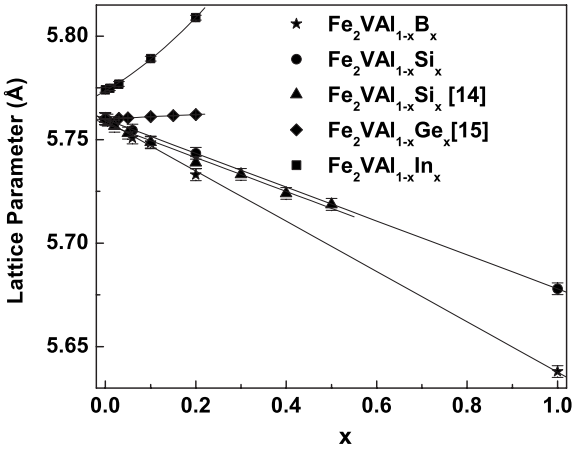

FIG. 2. Variation of lattice parameters as a function of composition x in $Fe_2VAl_{1-x}B_x$, $Fe_2VAl_{1-x}Si_x$, $Fe_2VAl_{1-x}In_x$, and $Fe_2VAl_{1-x}Ge_x$ alloys. The data on $Fe_2VAl_{1-x}Ge_x$ alloys are taken from Ref. 15.

erties of the Fe_2VAl system by comparing the transport properties of B and In-substituted alloys with Si-substituted alloys. In this paper, we report the structural and temperature variations of electrical transport properties (ρ and S) of a series of $Fe_2VAl_{1-x}B_x$ alloys with $x=0-1$ and compare these properties with In-, Si-, and Ge-substituted alloys.

II. EXPERIMENT

The alloy ingots of $Fe_2VAl_{1-x}B_x$ $(0 \leq x \leq 1)$ were prepared with a high purity elemental constituents using an arc-melting furnace under argon atmosphere. Melting was carried out several times in order to homogenize the samples. The samples were cut from the ingots and sealed in an evacuated quartz tubes at 1273 K for 48 h and then quenched in cold water. The samples were structurally characterized by powder x-ray diffraction (XRD) with Cu K_a radiation. Nominal composition assigned to each sample was regarded as accurate because the weight loss was found to be less than 0.3%. The electrical resistivity (ρ) and magnetoresistance (MR) of samples were measured using a standard dc four-terminal method in the temperature range of 3–300 K, using a cryogen free superconducting magnet up to the fields of 50 KOe. The Seebeck coefficient (S) was measured using a homemade apparatus over the temperature range of 15–300 K.[17]

III. RESULTS AND DISCUSSION

The x-ray diffraction patterns of the $Fe_2VAl_{1-x}B_x$ $(0 \leq x \leq 1)$ alloys were identified to form a single phase with cubic $L2_1$ structure. The overall XRD patterns remain the same on replacement of Al by B atom. As a typical case, the XRD patterns of Fe_2VAl and alloys in which 20% of Al is replaced by B, Si, and In atoms are depicted in Fig. 1. The data points were scanned at an interval of step width, $2\theta=0.01^0$, and analyzed with a Reitveld structural analysis using the refinement code FULLPROF program, which is also shown in the same figure. All samples exhibit a cubic structure with $Fm3m$ space group and with strong reflections at (200), (220), (400), and (422). As shown by the residues in the figure, the quality of the Reitveld fitting is good. Although the over all XRD patterns are similar for Fe_2VAl and its alloys with B, Si, and In substituents, the intensity of the peaks is found to increase with the In substitution while it diminishes with the B and Si substitutions as expected. B, Al, and In atoms are in the same group with different periods while Si is in the same period of Al with a different group in the periodic table. Furthermore, within the same group, the atom having the largest period has the thickest electron shell and the largest atomic radius, resulting in the largest lattice spacing, when they form the same type of alloy. Hence the lattice spacing of In-substituted alloy is larger in comparison to the Fe_2VAl alloy while it is smaller in case of B-substituted alloys. The variation of the lattice parameters as a function of compositions of B, Si, In, and Ge are shown in the Fig. 2. The lattice parameters obtained from the above data analysis decrease linearly with the increasing B concentration. A similar trend is also drawn in the Si-substituted Fe_2VAl system. On the other hand, the lattice parameter increases with the increase of In concentration and is of similar nature in the Ge-substituted alloys, as reported by Nishino *et al.*[15] Hence, B, Si, and In atoms are believed to occupy preferentially the Al sites according to Vegards' law, and this is attributed to the fact that the ionic radius of B and Si atoms are smaller than Al while In is larger.

The observed large electrical resistivity value ($\sim 10^3$ $\mu\Omega$ cm) at low temperatures and negative TCR for Fe_2VAl are shown in Fig. 3(a), and these results are in agreement with the earlier reports.[12–15] The sharp upturn in the low-temperature range ($3\ \text{K} < T < 20\ \text{K}$) could be fitted to variable-range hopping conduction behavior, $\ln(\rho) \alpha T^{-1/4}$; while at higher temperatures, a simple power law ($T^{3/2}$ dependence) follows [see insets of Fig. 3(a)]. On the basis of

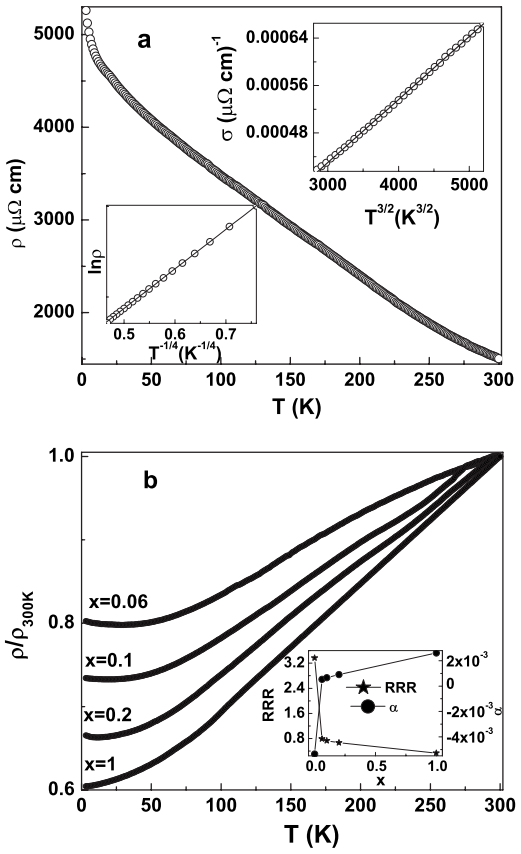

FIG. 3. (a) Temperature variation of electrical resistivity of the Fe_2VAl ($x=0$) alloy. Insets: Plots of ln ρ vs $T^{-1/4}$ and $s(T)$ vs $T^{3/2}$. (b) Normalized values of electrical resistivity as a function of temperature for $Fe_2VAl_{1-x}B_x$($x=0-1$) alloys.

our results, Fe_2VAl can be regarded as the zero-band gap semiconductor, which is consistent with the results of infrared reflectance data[10] and the theoretical predictions of narrow band gap.[9] A minute amount of B substitution for Al causes a sharp decrease in electrical resistivity and the sign of TCR changes from negative to positive. Intermediate compositions develop a low-temperature minimum in $\rho(T)$ curves below 50 K followed by a linear behavior: a typical behavior for ordinary metals. Finally for $x=1$, the low temperature minimum disappears and the obtained values of ρ are comparable to that of conventional intermetallic alloys. Anomalies observed in the $\rho(T)$ curves for $x>0$ alloys are barely discernible when plotted together on the same scale. Therefore, normalized resistivity $\rho(T)/\rho(300\ \mathrm{K})$ as a function of temperature is plotted for $x>0$ alloys in Fig. 3(b). The net change in resistance with temperature for a particular sample can be estimated by residual resistivity ratio (RRR) $\{=\rho(3\ \mathrm{K})/(\rho(300\ \mathrm{K})\}$, which is plotted as a function of B concentration along with the values of the temperature coefficient of resistivity, $\alpha=1/\rho(d\rho/dT)$, at 300 K [shown in the inset of Fig. 3(b)]. For all the alloys, the value of α lies in the range of $-5.35\times10^{-3}\ \mathrm{K}^{-1}$ ($x=0$) to $2.6\times10^{-3}\ \mathrm{K}^{-1}$ ($x=1$).

All the above discussed features suggest a semiconductor-like to metal transition on the substitution of B in place of Al. As the temperature is lowered from 300 K, the ρ decreases and goes through a minimum at temperatures ($T_{\min}$) below 50 K. The minimum developed in $\rho(T)$ curve could be due to the coexistence of negative TCR ($x=0$) and positive TCR ($x=1$) components in the intermediate compositions. As the B content increases, the positive TCR component dominates and results in the shift of $T_{\min}$ to lower temperatures. It is important to point out here that with the substitution of In, Si, and Ge in the Fe_2VAl system, such minimum in the $\rho(T)$ has not been observed.[12–15] This suggests that the B substitution results in two competing scattering mechanisms, one of which is responsible for the negative TCR and the other is for the positive TCR.

It is well established that the Fe_2VAl is nonmagnetic. Magnetization data on B-substituted Fe_2VAl shows that as the B content increases, a ferromagnetic component develops and large magnetization values have been observed for the alloy.[18] These results suggest that as the B content increases, a metallic and strong magnetic phase develops, therefore, it appears that the $T_{\min}$ is connected with the existence of localized moments induced by the magnetic impurities, indicating a characteristic signature of Kondo-scattering mechanism that can result in the low-temperature resistivity minimum. In many situations, low-temperature minimum is caused by the Kondo effect, which was originally encountered in nonmagnetic systems with a minute magnetic impurity.[19] Recently a similar effect was also found in strongly correlated manganites, as well as ferromagnetic metals.[20,21] According to Kondo's theory, the relation between electrical resistivity and temperature can be expressed by the formula $\rho_k=\rho_0+\rho_S \ln T$ below $T_{\min}$. Here, ρ_0 is the residual resistivity independent of temperature, the second term is the contribution from the interaction between localized magnetic moments and the conduction electrons, and the parameter ρ_s describes the strength of the spin scattering. Figure 4(a) shows the resistivity as a function of ln T for $x>0$ alloys. It shows a good linear dependence on ln T at low temperatures, as shown by the solid lines. The inset of Fig. 4(a) points out that the value of $T_{\min}$ decreases with B content. This behavior at low temperatures suggests that the spin scattering is weakened with the increase of B content.

If negative TCR is dominated by the Kondo effect, the spin scattering of conduction electrons should be distinctively suppressed by an external magnetic field. In order to check the validity of the Kondo mechanism, the resistivity measurements were carried out under an external magnetic field of 5 tesla. As a typical case, the results of $\rho(T)$ for $x=0.06$ alloy (with and without field) are shown in Fig. 4(b). It can be seen that the external field has a suppressing effect on the resistivity. In general, the slope, $\bar{\rho}_S=|\rho_{3\ \mathrm{K}}-\rho_{\min}|/|T_{3\ \mathrm{K}}-T_{\min}|$, of the curves below $T_{\min}$ is a representation of average strength of the magnetic scattering and directly proportional to ρ_S. The inset of Fig. 4(b) points out that the magnitude of the $\bar{\rho}_S$ below $T_{\min}$ decreases with increasing B content and the slope decreased with increasing magnetic field, indicating a weakened spin scattering. On the other hand, a low-temperature negative TCR may also arise in disordered systems from quantum interference effects such as weak localization.[22] However, the weak localization theory is generally applicable to the high resistivity ($\sim10^2\ \mu\Omega$-cm) systems. Furthermore, the ρ will be enhanced under a strong magnetic field. Thus, our low ρ values

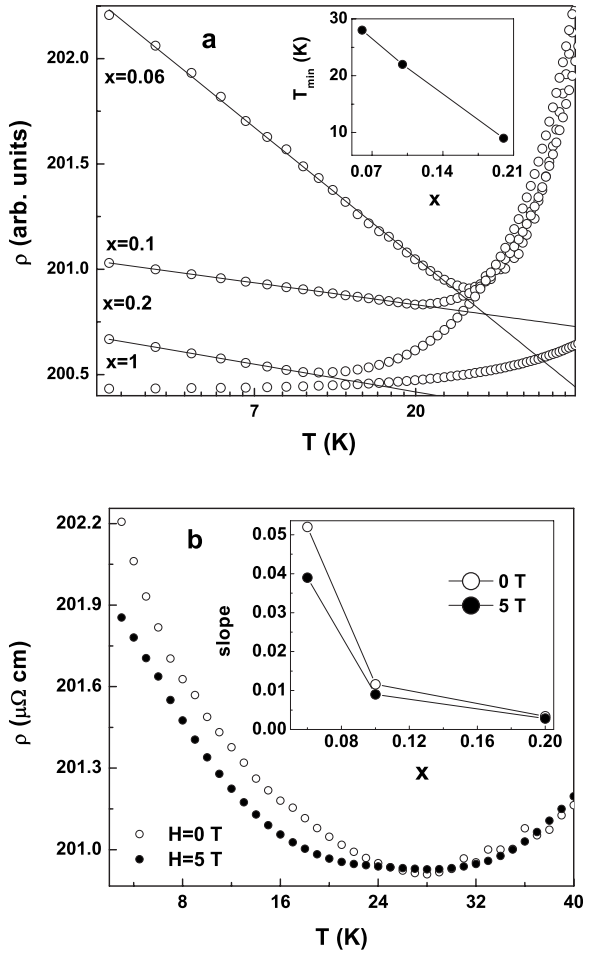

FIG. 4. (a) The electrical resistivity as a function of ln T for $Fe_2VAl_{1-x}B_x$ (x=0.06, 0.1, 0.2) samples in the temperature range of 3–80 K, which shows a good linear dependence on logarithmic temperature given by solid lines. The inset gives the plot of T_{min} vs x. (b) $\rho(T)$ curves at zero field and an external magnetic field of 5 T for the x=0.06 alloy. The inset shows the change of slope with variation of B concentration with and without external magnetic fields.

and small negative magnetoresistance rules out the possibility of any significant electronic disorder in the system that can give rise to localization effects. Therefore, we believe that the Kondo effect in the negative TCR range may play a significant role. Now we turn our attention to the positive TCR component of the resistivity. It is observed that the positive TCR component increases linearly above the T_{min} with increasing temperatures. The linear $\rho(T)$ behavior above T_{min} could be attributed to electron–phonon interaction[23] in the frame work of the Boltzmann transport theory using Bloch–Gruneisen (BG) formula that may be implemented as follows:

$$\rho(T) = \rho_2\left(\frac{T}{\Theta_D}\right)^n \int_0^{\Theta_D/T} \frac{x^n}{(e^x-1)(1-e^{-x})}dx. \quad (1)$$

The temperature dependent part of the resistivity, ρ_2, arises from the electron–phonon interactions and the exponent term "n" generally takes the values of 2, 3 and 5, depending on the nature of the interactions. For metallic systems that undergo magnetic ordering, the n values are taken to be 2 while n=3 is found in many nonmagnetic host d metals containing a number of impurities. n=5 is observed for nonmagnetic elements such as Cu, Ag or Au with a reasonable mean free path.[24] The decrease in ρ_0 and T_{min} may be taken as a signature of metallic and magnetic characters on B substitution. The BG contribution is expected to increase over the spin scattering as B increases.

For $T<10\Theta_D$, an accurate analytical expression of the integral in Eq. (1) (Ref. 25) can be simplified as follows:

$$\int_0^{\Theta_D/T} \frac{x^n}{(e^x-1)(1-e^{-x})}dx = \sum_{k=1}^{\infty} \int_0^{\Theta_D/T} x^n e^{-kx}dx. \quad (2)$$

Since the experimental value of Θ_D for the parent alloy is ~570 K,[1] we are justified in using Eq. (2) for $x>0$ alloys in the measured temperature range.

Furthermore, we examine quantitatively our assumptions of the coexistence of negative and positive TCRs for the intermediate compositions. Therefore, finally from the Matthiessen's rule, the total resistivity in the whole temperature range of the present study can be written as

$$\rho(T) = \rho_0 + \rho_1 \ln T + \rho_2\left(\frac{T}{\Theta_D}\right)^n \sum_{k=1}^{\infty} \int_0^{\Theta_D/T} x^n e^{-kx}dx. \quad (3)$$

The first term ρ_0 is the residual resistivity independent of temperature, the second term represents temperature dependent spin scattering, and the last term arises from the electron–phonon interaction. Now the $\rho(T)$ in the whole temperature range has been fitted to the Eq. (3) with n, ρ_1, ρ_2, and Θ_D as the free parameters. A best fit to the data in the wide temperature range, $3<T<220$ K, is obtained with n =3, as shown by the solid lines in the Fig. 5. The insets of the figure show the same resistivity plots with the temperature axis in a logarithmic scale in order to emphasize the quality of the fits in low-temperature regime. The coefficients of the individual scattering mechanisms in every term are tabulated in Table I. The values of ρ_0 and Θ_D for all the samples obtained from the above analysis were found to decrease systematically as the B content increases. It also shows that the intensity of the Kondo scattering decreases with the increase of content. However, we noticed that the effect of electron–phonon interaction term (ρ_2) is much larger than the Kondo interactions. The ρ_1 term is three orders smaller in magnitude than the ρ_2 term and decreases with the B content. We, therefore, conclude that the $\rho(T)$ with the B substitution is dominated by the electron–phonon interactions for the higher B content alloys, which leads to a conventional metallic system.

Now we turn our attention to noting the differences in ρ and its temperature dependence on the substitution of elements. Figure 6 shows an effect on ρ that was measured at 300 K as a function of the compositions in B-, In-, Si-, and Ge-substituted Fe_2VAl alloys. As a typical case, temperature variation of the normalized resistivity values of alloys, in which 20% of Al is replaced by B, Si, and In atoms, are

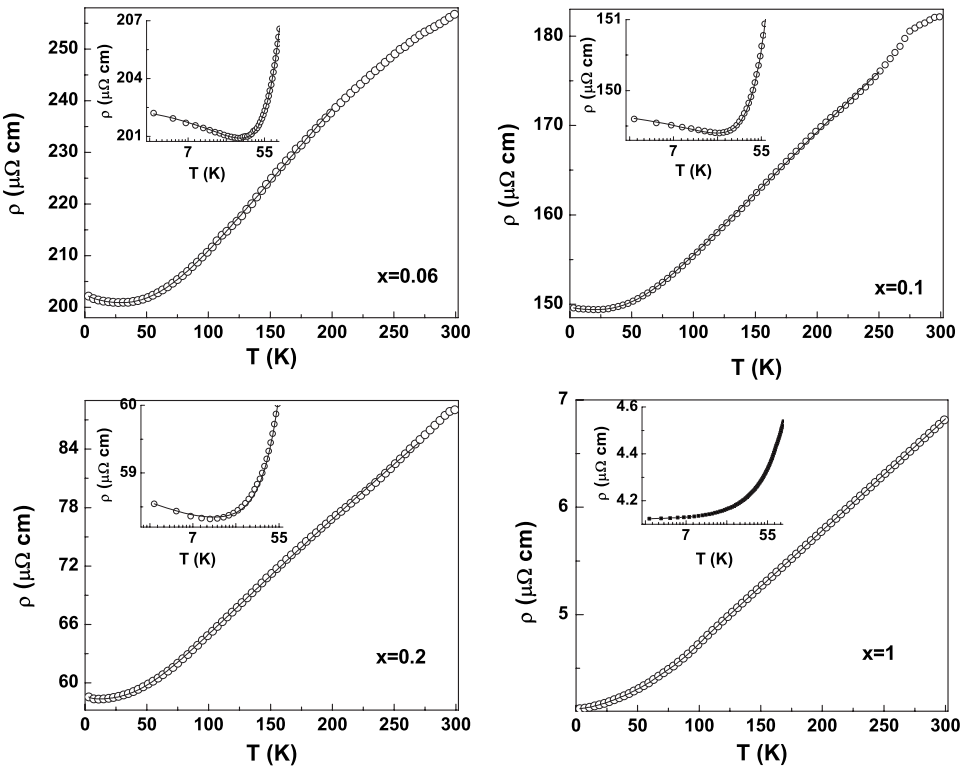

FIG. 5. Electrical resistivity as a function of temperature for $x>0$ alloys along with the fits to the Eq. (3) (see text) represented by solid lines. The inset shows the resistivity with the temperature axis in a logarithmic scale of the respective sample in order to show more clearly the low-temperature behavior of the resistivity.

depicted in the inset of Fig. 6. From the comparative study of ρ and its temperature dependence of B-, In-, Si-, and Ge–substituted Fe_2VAl alloys, we draw the following interesting features: (i) In all the samples [i.e., $Fe_2VAl_{1-x}M_x$ (M=B, In, Si, and Ge) alloys], the negative TCR turns to positive TCR with the substitution of quaternary elements. However, unlike the B-containing alloys, the $\rho(T)$ curves of the In, the Si, and the Ge containing alloys didn't show any low-temperature minimum. (ii) The absolute values of ρ decreases rapidly with even a minute substitution of the elements, which is believed to be semiconductorlike to metal transition. (iii) Other transport properties, i.e., S and MR, show distinct properties. The reduction in ρ on the substitution of Si and Ge is attributed to an increase in electron density, as Si and Ge atoms have additional electrons in comparison to that of Al. However, the similar trend of ρ with even an isoelectronic substitution is also obtained. However, the decrease in ρ is sharper for B-substituted alloys among all other substituents. Therefore, it indicates that the size of the atom also plays an important role in reducing the values of ρ. The origin of the crossover of TCR (from positive to negative) and the sensitivity of the electrical resistivity (which in turn is a measure of conductivity) with the substitution of elements appear to be related to the band-structure modification.

TABLE I. Parameters obtained from the experimental data corresponding to the fit to the Eq. (3) (see text) for $Fe_2VAl_{1-x}B_x$ ($x>0$) alloys: resistivity units are in ($\mu\Omega$ cm) and Θ_D in K.

x	ρ_0	ρ_1	ρ_2	Θ_D
0.06	203.5	0.9828	241.82	485
0.1	149.8	0.8057	112.40	452
0.2	58.66	0.03668	61.497	381
1	4.099	0.0005	7.606	347

The temperature dependence of Seebeck coefficient, $S(T)$, is more sensitive than the temperature dependence of electrical conductivity to the variation in the energy spectrum near the Fermi level. Therefore, $S(T)$ provides a complementary information about the electronic band structure near the Fermi level. In view of this, we measured the $S(T)$ of $Fe_2VAl_{1-x}B_x$ (x=0–1) alloys and the results are shown in Fig. 7(a). The stoichiometric Fe_2VAl composition exhibits positive values of S in the whole temperature range of the

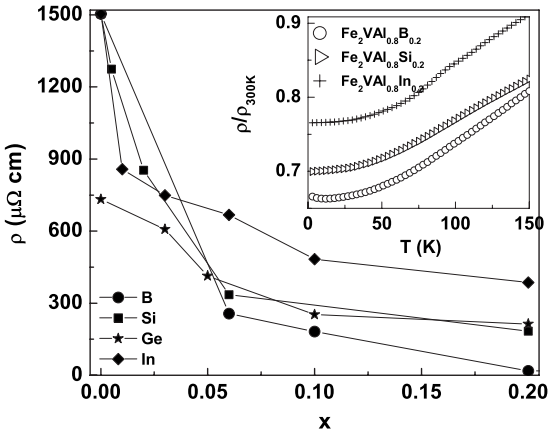

FIG. 6. Electrical resistivity at 300 K as a function of composition x in $Fe_2VAl_{1-x}B_x$, $Fe_2VAl_{1-x}Si_x$, $Fe_2VAl_{1-x}In_x$, and $Fe_2VAl_{1-x}Ge_x$ alloys. The data on $Fe_2VAl_{1-x}Ge_x$ alloys are taken from Ref. 15. Inset: Normalized values of electrical resistivity as a function of temperature for $Fe_2VAl_{0.8}B_{0.2}$, $Fe_2VAl_{0.8}Si_{0.2}$, and $Fe_2VAl_{0.8}In_{0.2}$ alloys.

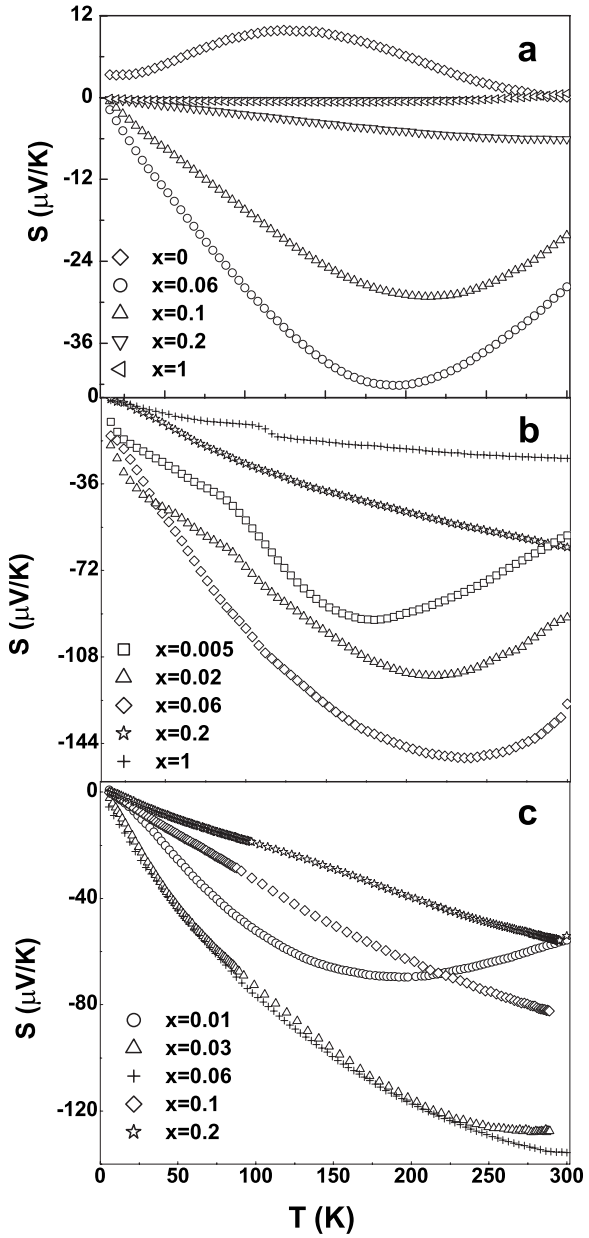

FIG. 7. Temperature variation of Seebeck coefficient of (a) $Fe_2VAl_{1-x}B_x$, (b) $Fe_2VAl_{1-x}Si_x$, and (c) $Fe_2VAl_{1-x}In_x$ alloys.

present study with a broad maximum in the $S(T)$ curves around 120 K. The positive values of S (~ 10 μV/K) indicate that this alloy has a low carrier density with excess holes relative to electrons, being consistent with the earlier reports.[12–14] The downturn of S at high temperatures is attributed to the contribution of thermally excited carriers across the energy gap. When a small amount of Al is replaced by B, a drastic change in both magnitude and sign of S is observed. As B content increases from 0 to 1, the value of S at 300 K changes from +5 μV/K to a minimum of −24 μV/K for $x=0.06$ and eventually returns to a small positive value of 0.6 μV/K for $x=1$. The absolute value of S increases as the temperature increases and passes through a broad maximum, which is found to shift toward higher temperatures as the B content is increased. A similar $S(T)$ behavior has also been

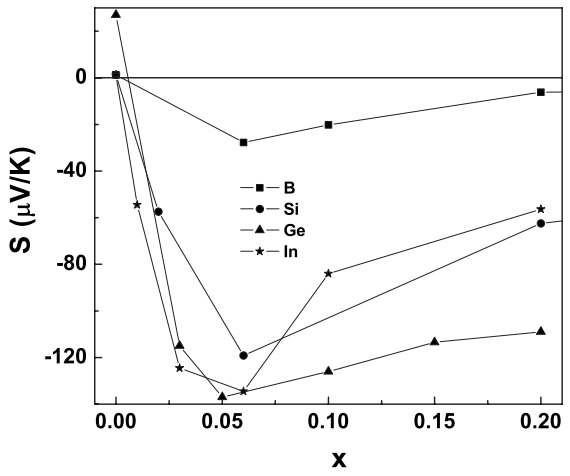

FIG. 8. Seebeck coefficient at 300 K as a function of composition x in $Fe_2VAl_{1-x}B_x$, $Fe_2VAl_{1-x}Si_x$, $Fe_2VAl_{1-x}In_x$, and $Fe_2VAl_{1-x}Ge_x$ alloys. The data on $Fe_2VAl_{1-x}Ge_x$ alloys are taken from Ref. 15.

observed in Si- and In-substituted alloys but with larger values of S, as shown in Figs. 7(b) and 7(c), respectively. The maximum value of $|S|$ obtained in the case of $Fe_2VAl_{1-x}Si_x$($x=0-1$) alloys is 150 μV/K for $x=0.06$ composition while it is 134 μV/K for $x=0.06$ composition in the case of $Fe_2VAl_{1-x}In_x$($x=0-0.2$) alloys. The results obtained in the Si-substituted alloys are well in agreement with the earlier reports.[13,14] Furthermore, similar $S(T)$ behavior has also been observed in recently reported Ge-substituted alloys[15] and also for the off-stoichiometric $(Fe_{2/3}V_{1/3})_{100-y}Al_y$ alloys.[26] In order to understand the role of substitution of the isoelements (B and In) and (Si and Ge) in Fe_2VAl, the value of S at 300 K as a function of compositions are plotted in Fig. 8. The positive values of S for Fe_2VAl change to large negative values irrespective of the doping elements. It is important to point out that the values of S change more drastically in the cases of In, Si, and Ge in comparison to B–substituted Fe_2VAl alloys. The reason for obtaining large values of S in Si- and Ge-substituted alloys is probably because of an increase in electron density. As suggested by Nishino *et al.*,[15] with the increase in electron density (on substitution of Si/Ge), the E_F moves from one side of the gap to the other, resulting in large changes in the S values. On the other hand, similar argument cannot be justified for the large changes obtained in S with the isoelectronic elemental (In) substitution for Al in Fe_2VAl alloy. Therefore, it is possible that by varying atomic sizes (with the substitution of B/In atoms), the characteristics of pseudogap changes although the position of E_F remains at same place; thereby, the large values of S are obtained with the substitution of larger In atom and smaller values of S are obtained with the substitution of smaller B atom.

Although the isostructural alloy Fe_2VGa is having a similar electronic structure of Fe_2VAl, the value of S is found to be large positive compared to Fe_2VAl. Hybridization between $3d$ states of Fe, V and sp states of Z elements were responsible for such differences in the S values. In a similar manner, the small negative values of S for B-substituted alloys and large negative values of S for In-substituted alloys

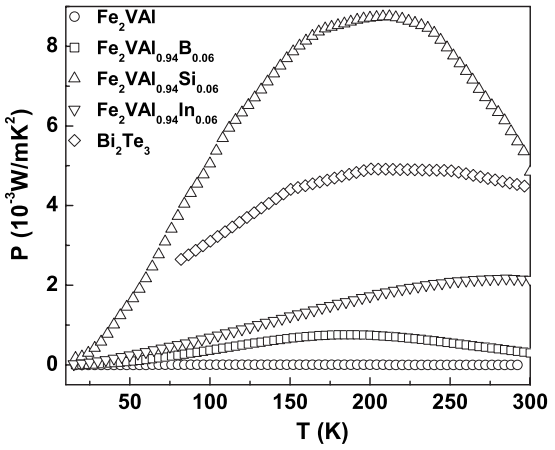

FIG. 9. Power factor as function of temperature for Fe_2VAl, $Fe_2VAl_{0.94}B_{0.06}$, $Fe_2VAl_{0.94}Si_{0.06}$, and $Fe_2VAl_{0.94}In_{0.06}$ alloys at 300 K

may also be due to the weak/strong hybridization between the Fe-3*d* and the *Z*-2*p* states, resulting in the overlap of bands, which in turn decides its metallic nature and the values of *S*. Unfortunately, at present, no detailed band-structure calculations are available on B- and In-substituted Fe_2VAl alloys. However, our results can be supported by band-structure calculations on Fe_2MnZ [*Z*=Al, Si, P] alloys,[16] which suggest that the *Z* atom influences the electronic character of the system through hybridization of $Z-p$ states with Fe and Mn *d states.* Similarly, it can be considered that the hybridization between *sp* states of B/In and Al atoms, and 3*d* states of Fe and *V* atoms may play a role in the formation of electronic band structure, resulting in such transport properties. Therefore, we suggest that the substitution of isoelectronic elements is also responsible for drastic changes in the transport properties unlike the interpretations given in the Si- and Ge-substituted alloys. Thus, the lower values of ρ are obtained for the B substitution while higher values of $|S|$ are obtained by the substitution of tetravalent elements such as Si and Ge, and a larger atom, In. This clearly indicates that the DOS near the E_F of Fe_2VAl alloy is sensitive to the substitution of elements. Therefore, the DOS at E_F dictates the electrical transport behavior by either altering the characteristics of pseudogap (by varying the atomic sizes) or the position of E_F (by changing the electron density).

Materials having a combination of lower ρ and higher *S* values can be promising candidates for the potential thermoelectric applications. The efficiency of these materials can be measured by its power factor, *P*, which is proportional to the S^2/ρ. The obtained values of *P* for Fe_2VAl is only of the order of 3×10^{-5} W/mK^2. However, a rapid increase in *P* is observed with a minute substitution of B, In, and Si atoms. For the Si-substituted alloys, the *P* values increase by two orders of magnitude (i.e., $\sim5\times10^{-3}$ W/mK^2), as high as conventional thermoelectric materials such as Bi_2Te_3. As shown in Fig. 9, we have also plotted the temperature variation of power factor of $Fe_2VAl_{0.94}Si_{0.06}$, $Fe_2VAl_{0.94}In_{0.06}$, $Fe_2VAl_{0.94}B_{0.06}$, and Fe_2VAl alloys along with the Bi_2Te_3 alloy for comparison. Among the various compositions of substitution elements, the maximum value of power factor (4.84×10^{-3} W/mK^2 at 300 K) is obtained for $Fe_2VAl_{0.94}Si_{0.06}$ which appears to be a promising candidate for potential thermoelectric applications at room temperatures. At intermediate temperature the power factor observed is even more than the conventional thermoelectric materials. This prompts us to suggest that these materials can be potential candidates for thermoelectric power applications in space vehicles operating at cryogenic temperatures. It is worth mentioning that a recent study of Ge-substituted Fe_2VAl alloys showed a significant improvement of *P* up to 5.9×10^{-3} W/mK^2 at 300 K for $Fe_2VAl_{0.9}Ge_{0.1}$ alloy, which is comparable to our presently studied/optimized $Fe_2VAl_{0.94}Si_{0.06}$ alloy. The large values of power factor observed in these alloys are similar to that of narrow band gap semiconductors. The similarities between the present alloy system and narrow band gap alloys suggest that the band-structure of these materials might be alike. Further studies with optimum substitutions in Fe_2VAl based alloys may provide materials that are competent enough to replace the presently used thermoelectric materials and also to understand the band structure.

The above discussed results give an empirical evidence of semiconductorlike to metal transition in the $Fe_2VAl(B)$ alloy system. Furthermore, these results also suggest that the lattice parameter changes observed (from the structural data analysis) due to atomic size differences between the substituted atoms also play an important role in modifying the electronic behavior of Fe_2VAl. In other words, it suggests that chemical pressure induces changes in electronic properties. Therefore, the study of electrical transport behavior under applied pressures would be helpful to confirm this idea. Similarly extensive band-structure calculations would certainly provide more guidance in the advancement and understanding of these materials.

IV. CONCLUSIONS

Structural and electrical transport behavior of intermetallic $Fe_2VAl_{1-x}B_x$ ($x=0-1$) alloys have been reported. From the structural analysis, it is confirmed that the B-substituted Fe_2VAl alloys stabilize in the Heusler-type with isostructural $L2_1$ phase. We report that the B substitution in Fe_2VAl has been attempted and is shown to form $L2_1$ phase. The temperature dependence of electrical transport properties such as resistivity (with and without the applied magnetic field) and Seebeck coefficient of $Fe_2VAl_{1-x}B_x$ ($x=0-1$) alloys have been investigated and the following conclusions are drawn from the study:

(i) From the temperature dependence of resistivity data analysis, it has been shown that a zero-band gap semiconductorlike behavior (for $x=0$) changes to conventional metallic state (for $x=1$).

(ii) At intermediated compositions (e.g., $x=0.06$) a low-temperature anomaly in $\rho(T)$ has been observed, which is explained using Kondo-type scattering mechanism at low temperatures and a dominant electron–phonon contribution at higher temperatures.

(iii) From the comparative study of transport behavior on

isoelectronic (B and In) and nonisoelectronic (Ge and Si) substitutions in place of Al, it is now suggested that although the electronic density plays a role in altering the electronic transport properties, the atomic size and hybridization effects also play a significant role in altering the physical properties of Fe_2VAl.

(iv) Low electrical resistivity coupled with high Seebeck coefficient result in higher thermoelectric power factor values in all the samples investigated in the present study.

(v) The doping of B atom is more effective in reducing the electrical resistivity while the Si substitution is more effective in increasing the S values. Hence, with the optimum substitutions in Fe_2VAl based alloys, one can tune to produce lower ρ and higher S values, which are essential to make them competent enough to replace the presently used thermoelectric materials.

ACKNOWLEDGMENTS

The financial assistance provided by the Council of Scientific and Industrial Research, India, is gratefully acknowledged. The support from DST-FIST for low-temperature work is also acknowledged.

*Corresponding author. FAX:+91-3222-255303.veeturi@phy.iitkgp.ernet.in

[1] Y. Nishino, Intermetallics **8**, 1233 (2000).
[2] Y. Nishino, M. Kato, S. Asano, K. Soda, M. Hayasaki, and U. Mizutani, Phys. Rev. Lett. **79**, 1909 (1997).
[3] G. Y. Guo, G. A. Botton, and Y. Nishino, J. Phys.: Condens. Matter **10**, L119 (1998).
[4] K. Ooiwa and K. Endo, J. Magn. Magn. Mater. **177-181**, 1443 (1998).
[5] E. Popiel, M. Tuszynski, W. Zarek, and T. Rendecki, J. Less-Common Met. **146**, 127 (1989).
[6] C. S. Lue and J. H. Ross, Phys. Rev. B **58**, 9763 (1998); **61**, 9863 (2000).
[7] Y. Feng, M. V. Dobrotvorska, J. W. Anderegg, C. G. Olson, and D. W. Lynch, Phys. Rev. B **63**, 054419 (2001).
[8] M. Kato, Y. Nishino, S. Asano, and S. Ohara, J. Jpn. Inst. Met. **62**, 669 (1998).
[9] R. Weht and W. E. Pickett, Phys. Rev. B **58**, 6855(1998); M. Weinert and R. E. Watson, *ibid.* **58**, 9732 (1998).
[10] H. Okamura, J. Kawahara, T. Nanba, S. Kimura, K. Soda, U. Mizutani, Y. Nishino, M. Kato, I. Shimoyama, H. Miura, K. Fukui, K. Nakagawa, H. Nakagawa, and T. Kinoshita, Phys. Rev. Lett. **84**, 3674 (2000).
[11] G. A. Botton, C. J. Humphreys, and Y. Nishino, Intermetallics **8**, 1209 (2000).
[12] M. Vasundhara, V. Srinivas, and V. V. Rao, J. Phys.: Condens. Matter **17**, 6025 (2005).
[13] Y. Nishino, Mater. Sci. Forum **449-452**, 909 (2004).
[14] C. S. Lue, C. F. Chen, J. Y. Lin, Y. T. Yu, and Y. K. Kuo, Phys. Rev. B **75**, 064204 (2007).
[15] Y. Nishino, S. Deguchi, and U. Mizutani, Phys. Rev. B **74**, 115115 (2006).
[16] S. Fujii, S. Ishida, and S. Asano, J. Phys. Soc. Jpn. **64**, 185 (1995).
[17] M. Vasundhara, V. V. Rao, and V. Srinivas, Ind. J. Cryogenics **31**, (1-4) 116 (2006).
[18] M. Vasundhara (unpublished).
[19] J. Kondo, Prog. Theor. Phys. **32**, 37 (1964).
[20] J. Zhang, Y. Xu, S. Cao, G. Cao, Y. Zhang, and C. Jing, Phys. Rev. B **72**, 054410 (2005).
[21] A. N. Pasupathy, R. C. Bialczak, J. Martinek, J. E. Grose, L. A. K. Donev, P. L. Mceuen, and D. C. Ralph, Science **306**, 86 (2004).
[22] P. W. Anderson, E. Abrahams, and T. V. Ramakrishnan, Phys. Rev. Lett. **43**, 718 (1979); B. L. Al'tshuler and A. G. Aronov, Sov. Phys. JETP **50**, 968 (1979); G. Bergmann, Phys. Rev. B **28**, 2914 (1983).
[23] J. M. Ziman, *Electron and Phonons* (Clarendon, Oxford, 1960).
[24] Y. Y. Tsiovkin, M. A. Korotin, A. O. Shorikov, V. I. Anisimov, A. N. Voloshinskii, A. V. Lukoyanov, E. S. Koneva, A. A. Povzner, and M. A. Surin, Phys. Rev. B **76**, 075119 (2007).
[25] M. Deutsch, J. Phys. A **20**, L811 (1987).
[26] Y. Nishino, H. Kato, M. Kato, and U. Mizutani, Phys. Rev. B **63**, 233303 (2001).